UNIVERSITY OF BATH

University of Bath

Illumination of mesospheric irregularity by lightning discharge

Martin Füllekrug,[1] Andrew Mezentsev,[1] Serge Soula,[2] Oscar van der Velde,[3] and Adrian Evans[1]

[1] Theoretical model calculations recently predicted the existence of mesospheric irregularities which assist the initiation of sprites. Here we report the experimental detection of a ∼3–19 km^3 large mesospheric irregularity at ∼80–85 km height which is illuminated by the electromagnetic field of an intense positive cloud-to-ground lightning discharge. While the lightning discharge causes a prompt group of four sprites above the lightning discharge, the mesospheric irregularity is found at a horizontal distance at least ∼15–20 km away from the sprite group and it rebrightens ∼40–60 ms after the sprite group occurrence. This rebrightening is driven by a local quasi-static electric field enhancement with a charge moment ∼4–20 C km which causes the irregularity to develop a downward descending luminous column from ∼75–85 km height. The quasi-static electric field enhancement is caused by the reorganization of residual charge inside the thundercloud during a high-level activity of intracloud discharges with ∼10–20 pulses per ms. Such mesospheric irregularities might have an effect on the wave propagation of 100 kHz radio waves which are used for atomic time transfer and marine navigation. **Citation:** Füllekrug, M., A. Mezentsev, S. Soula, O. van der Velde, and A. Evans (2013), Illumination of mesospheric irregularity by lightning discharge, *Geophys. Res. Lett.*, *40*, 6411–6416, doi:10.1002/2013GL058502.

1. Introduction

[2] Recent model calculations strongly suggest that enhancements of the electron density in the middle atmosphere are particularly effective in assisting the initiation of sprites below the conventional breakdown threshold [*Qin et al.*, 2013b, 2013a, 2012a, 2012b; *Kosar et al.*, 2012]. The initiation of sprites below the conventional breakdown threshold is currently under debate [*Liu et al.*, 2012] based on numerous compelling observations and numerical simulations of sprites [*Gamerota et al.*, 2011; *Li et al.*, 2008; *Hu et al.*, 2007]. The prediction that inhomogeneities in the

middle atmosphere could be illuminated by lightning electromagnetic fields is a major milestone for the maturing understanding of sprites because the physical mechanisms leading to sprite streamers might be used as a remote-sensing tool for the middle atmosphere in future studies. For example, sprites have already been used to infer the electric field strengths produced by a preceding gigantic jet [*Neubert et al.*, 2011]. Moreover, electron density inhomogeneities in the mesosphere might have a significant impact on the absorption and scattering of radio waves which will be used for the remote sensing of lightning discharges and sprites on the forthcoming TARANIS (Tool for the Analysis of RAdiations from lightNIngs and Sprites) satellite mission [*Lefeuvre et al.*, 2008; *Blanc et al.*, 2007]. An improved understanding of the proposed inhomogeneities in the middle atmosphere is therefore important for the preparation of the TARANIS mission, which is the aim of this contribution.

2. Observations

[3] Unstable air masses between France and Spain developed into a mesoscale convective system in the early evening hours of 16 August 2013 (Figure 1). The convective system reaches an extent of ∼300 × 300 km^2 around ∼20–21 UTC and covers the entire mountain range of the Pyrénées where numerous sprite occurrences have been predicted to occur [*Füllekrug and Reising*, 1998]. A positive lightning discharge with a peak current of ∼159 kA occurs at 20:27:58.721 UTC. Several other weak negative lightning discharges occur at scattered locations up to ±400 ms before and after the positive lightning discharge (not shown in Figure 1). The area above the mesoscale convective system is observed with a low-light video camera located in Clermont-Ferrand (45.8°N, 3.1°E, 400 m), ∼440 km northeast of the positive lightning discharge. This low-light video camera is a Watec 902H, which records video frames with 8 bit resolution using a fixed nonlinear (gamma) gain and stepped interlacing at an initial sampling frequency of 25 frames per second [*Soula et al.*, 2012]. The subsequent deinterlacing into even and odd fields during post-processing results in an image sequence with a temporal resolution of 20 ms as verified by meteor track observations. The camera records a prompt group of four carrot sprites (Figure 2a) in the image lasting from 20:27:58.718–58.738, which is synchronized to UTC with a GPS time inserter with an accuracy ∼1 ms. The sprite group occurs around the azimuth of the positive lightning discharge (Figure 1) as inferred from the video image with an accuracy ∼1 km [*van der Velde et al.*, 2010] by use of the software "Cartes du Ciel" (sky charts), which matches stars with those visible in the video image. The horizontal extent of the sprite group is estimated to be ∼30–40 km by using the distance between the camera and the positive lightning discharge.

---

[1]Centre for Space, Atmospheric and Oceanic Science, Department of Electronic and Electrical Engineering, University of Bath, Bath, UK.

[2]Laboratoire d'Aérologie, CNRS, Université de Toulouse, Toulouse, France.

[3]Department of Electrical Engineering, Technical University of Catalonia, Terrassa, Spain.

Corresponding author: M. Füllekrug, Centre for Space, Atmospheric and Oceanic Science, Department of Electronic and Electrical Engineering, University of Bath, Claverton Down, Bath BA2 7AY, UK. (M.Fullekrug@bath.ac.uk)
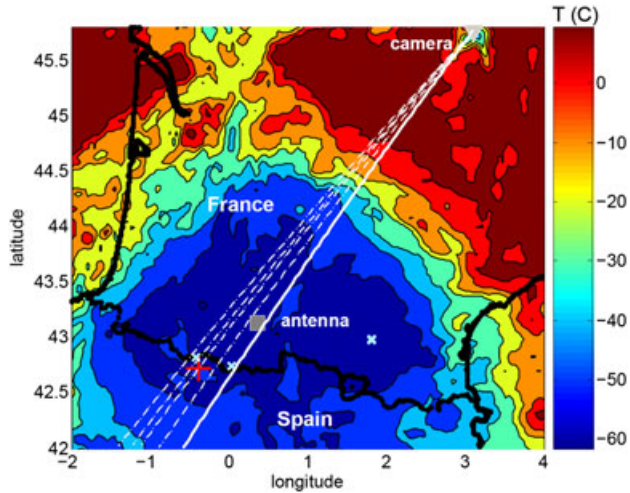
Figure 1. A mesoscale convective system with minimum cloud top temperatures $\sim -60°$C occurs above the Pyrénées between France and Spain and extends over $\sim 300 \times 300$ km^2 in the early evening hours of 16 August 2013. The area above the thunderstorm is observed with a low-light video camera located in Clermont-Ferrand (45.8°N, 3.1°E, gray triangle). An intense positive lightning discharge with a peak current of ~ 159 kA occurs at 20:27:58.721 UTC (red cross) and causes a group of four sprites (dash-dotted lines) and a small luminosity column (white solid line). A consecutive negative lightning discharge with a peak current ~ -6 kA occurs at 20:27:58.755 UTC (blue dot). A radio receiver ~ 77 km northeast of the positive lightning discharge (gray square) records the electric field strength during the sequence of events.

[4] To determine relative luminosities against the bright moonlit background during the entire video sequence, we make use of morphological image processing. The first step of the image processing is to determine the gray level distribution function for each image pixel to identify the 10% largest luminosities for each pixel in the video sequence of 1.08 s length, which corresponds to 54 images. The identified candidate pixels are typically disconnected such that a spatial filter is applied to define a contiguous image area.

Here we make use of a morphological image opening with a 3×3 pixel large square as a structuring element. The image opening removes the isolated regions that are smaller than the structuring element while leaving the larger regions relatively unaffected [*Gonzalez and Woods*, 2008, pp. 635–639]. The resulting contiguous areas are used as an image mask to extract those pixels from the original image, which have unusual large luminosities. The relative luminosity of the sprite is determined here as the excess luminosity above the median, calculated with respect to time for each individual image pixel (Figure 2b).

[5] The image processing makes the body of the four sprites between ~ 70 km and ~ 80 km height, the diffuse glow between ~ 80 km and ~ 90 km height, and the tendrils extending down to ~ 50 km height immediately apparent. The sprite group is surrounded by several patches of luminosity with unknown significance. Yet one patch to the left of the sprite group (Figure 2b) rebrightens ~ 40–60 ms after the occurrence of the sprite group, and the rebrightening is followed by the development of a descending column of luminosity, i.e., a small column sprite, which is clearly significant (Figure 2c). The initial patch has a width of ~ 1–2 km and extends over ~ 4–6 km occupying ~ 3–19 km^3 from ~ 80 to ~ 85 km height (Figure 2b), and it is located at least ~ 15–20 km to the left of the sprite group (Figure 1). This is a surprising result because the patch is completely disconnected from the diffuse glow above the sprite group. In other words, the electromagnetic field from the positive lightning discharge at 20:27:58.721 UTC was not sufficient to illuminate the area between the sprite group and the patch, but it was sufficient to illuminate the patch, which strongly indicates an irregularity of the ambient conditions in the volume of mesospheric air occupied by the patch. A weak negative lightning discharge with a peak current ~ -6 kA occurs at 20:27:58.755 UTC (Figure 1) and might have helped to initiate the rebrightening of the patch while other scattered lightning discharges occurring in the same area with similar peak currents (not shown in Figure 1) have no effect on the mesosphere above. The downward propagation speed during the rebrightening of the patch is estimated to be at least ~ 1.25–2.50$\cdot 10^5$ m s^{-1} by using a vertical distance of ~ 5 km (5 pixels) traveled in ~ 20–40 ms (1–2 images). Note that this extremely slow downward descent of the column sprite
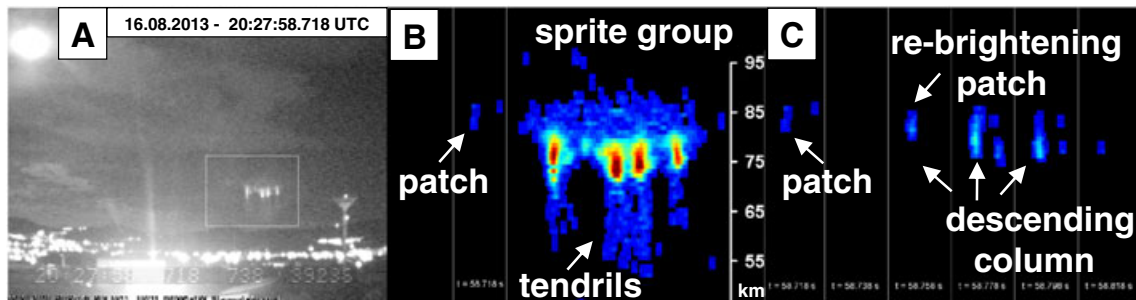

Figure 2. A descending column of luminosity appears after a group of four sprites recorded with the low-light video camera in Clermont-Ferrand. (a) The original video image shows a group of four sprites. Note that the sprite group was recorded against the full moon in the upper left corner of the video image. (b) The excess luminosity above the median of each pixel within the image mask exhibits a diffuse glow around ~ 80–90 km height above the body of the sprite group between ~ 70 and ~ 80 km and tendrils extending down to ~ 50 km height. A small patch of luminosity appears to the left of the sprite group between ~ 80 and ~ 85 km height. (c) This patch rebrightens at ~ 20:27:58.758 and develops subsequently into a column which descends down to ~ 74–76 km height from ~ 20:27:58.758 to 58.818.
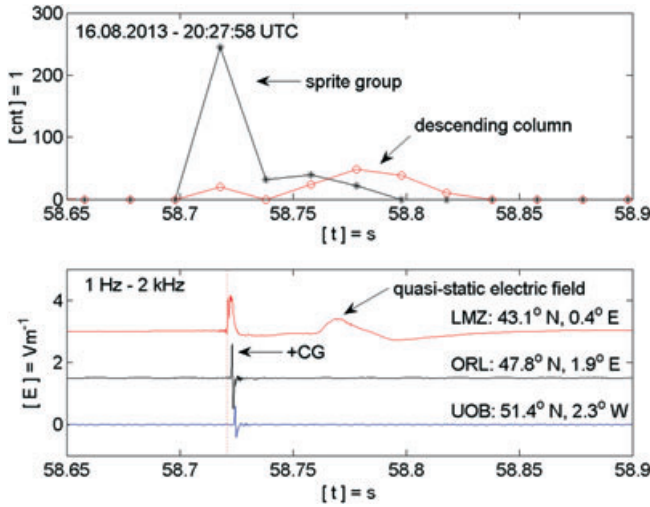
Figure 3. The descent of the column sprite is caused by a quasi-static electric field. (top) The relative luminosity of the descending column (red line) reaches its maximum ∼60 ms after the peak luminosity of the sprite group (black line) as inferred from the video recordings. (bottom) The sprite group is caused by a positive cloud-to-ground discharge (+CG) at 20:27:58.7208 (red dotted line) as measured with three radio receivers at ∼77 km (LMZ = Lannemezan, red line), ∼604 km (ORL = Orléans, black line), and ∼980 km (BTH = Bath, blue line) away from the lightning discharge in the frequency range from 1 Hz to 2 kHz. The nearest radio receiver ∼77 km from the sprite shows an increase of the electric field strength, which causes the descending column of luminosity. The enhancement of the electric field strength for ∼30 ms is not associated with electromagnetic radiation, which is detectable at the more distant radio receivers, and it is therefore attributed to a local quasi-static electric field. Note that the small time delays of the electromagnetic radiation from the +CG are caused by the wave propagation from the lightning discharge to the radio receivers.

is likely to require forcing by an additional electromagnetic field to occur.

[6] Vertical electric field strengths in the frequency range from ∼1 Hz to ∼400 kHz have been recorded with three wideband digital radio receivers near Lannemezan (43.1°N, 0.4°E), Orléans (47.8°N, 1.9°E), and Bath (51.4°N, 2.3°W) with a sampling frequency of 1 MHz, a resolution ∼1–2 μV m⁻¹ Hz⁻¹/², and a timing accuracy ∼12 ns [*Füllekrug*, 2010]. The electric field recordings in the frequency range from 1 Hz to 2 kHz are compared to the relative luminosities of the sprite group and the patch (Figure 3). The relative luminosities are calculated from the square root of the integrated luminosities above the median for each image pixel within their respective image masks as inferred from the video recordings with 20 ms resolution. The nonlinear gain of the video camera and the saturation of the sprite group are not considered here because the comparison between the relative luminosity and the electric field recordings is entirely based on their temporal evolution. The relative luminosity of the sprite group coincides with the radio signal from the positive lightning discharge. The luminosity from the rebrightening patch and the descending column coincides with an electric field enhancement starting at ∼20:27:58.760 UTC (Figure 3), i.e., ∼5 ms after the negative lightning

discharge with a peak current ∼–6 kA (Figure 1). The enhancement lasts for ∼25–30 ms, and it is only seen by the radio receiver in Lannemezan ∼77 km northeast of the positive lightning discharge. The radio receivers in Orléans and Bath are ∼604 km and ∼980 km away and do not exhibit the same electric field enhancement. It is therefore evident that this electric field enhancement results from a local quasi-static electric field which decays much faster with distance than the radiated electromagnetic field from the positive lightning discharge. The radiated field from the positive lightning discharge measured in Bath and Orléans indicates a charge moment change ∼200–230 C km, which is inferred from the transfer function between the observed and calculated electric field spectrum [*Füllekrug et al.*, 2006, equations 1 and 2] using the short pulse approximation of the normal mode expansion with frequency-dependent ionospheric heights [*Füllekrug and Rycroft*, 2006, equation 2] from 1 Hz to 200 Hz. The observed charge moment change is relatively small because no lightning continuing current appears to be present in the electric field recordings.

[7] A high level of discharge activity is superimposed on the quasi-static electric field in Lannemezan (Figure 4, top left). The discharge activity is measured in the frequency range from 40 kHz to 400 kHz, and it exhibits numerous brief pulses which occur at a rate of ∼10–20 per ms or ∼1–2 per 100 μs. The intensity of the pulses and their occurrence rate are used to characterize the electric field variability ΔE of the discharge activity by calculating for each 100 μs long time interval the logarithmic mean

$$\mu = \frac{1}{N} \sum_{k}^{N} \log_{10} S(f_k) \qquad (1)$$

where $S(f_k)$ are the spectral amplitude densities at $N = 37$ frequencies f_k from 40 kHz to 400 kHz separated by 10 kHz such that the electric field variability is finally given by $\Delta E = 10^{\mu}$. The agreement between the quasi-static electric field and the high-level discharge activity is excellent (Figure 4, top left and center left panels). A similar example of a high-level discharge activity superimposed on a quasi-static electric field (Figure 4, top right and center right panels) was observed in association with an extremely well-documented example of two consecutive lightning discharges [*Füllekrug et al.*, 2013b]. The source locations of the pulses occurring during the second lightning discharge have been mapped with an array of radio receivers [*Mezentsev and Füllekrug*, 2013] which shows that their origin are intracloud lightning discharges at an average height of ∼3.5 km (Figure 4, bottom). The similarity of the two examples recorded near Lannemezan and Rustrel strongly suggests that the high level of discharge activity recorded in Lannemezan also results from intracloud lightning discharges.

3. Interpretation

[8] The interpretation of the experimental results is straightforward. The cloud-to-ground lightning discharge removes positive charge from the thundercloud, which causes the prompt appearance of the sprite group. A disconnected mesospheric irregularity concentrates the electric field lines from the positive cloud-to-ground lightning discharge. In this way, the mesospheric irregularity causes a localized enhancement of the electric field strength which
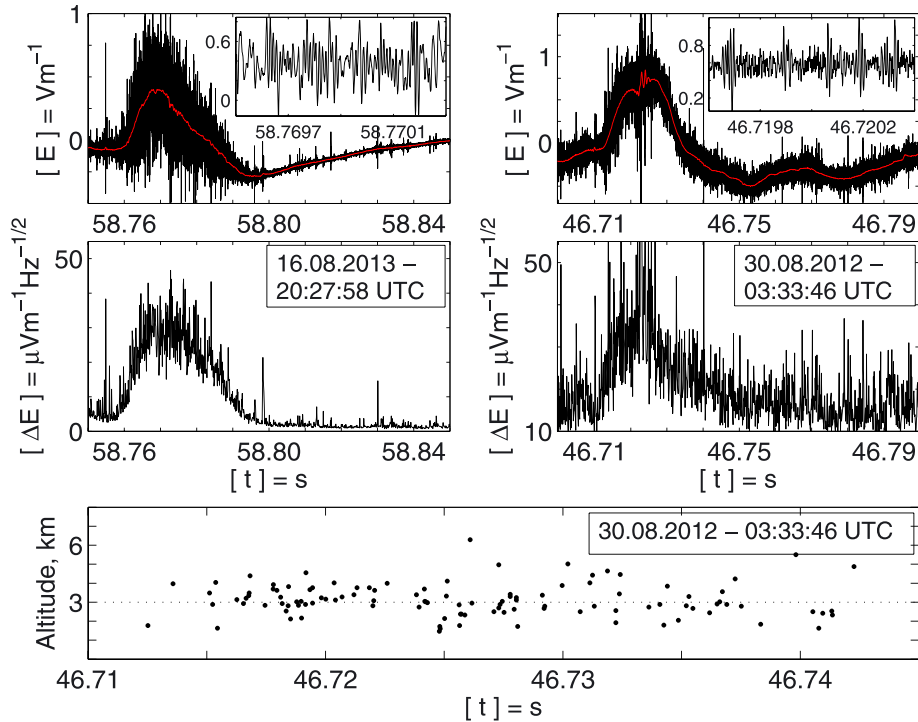
Figure 4. A high level of intracloud discharge activity is superimposed on the quasi-static electric field enhancement. (top) The high level of the discharge activity (black line) with ~1–2 pulses per 100 μs (inset) is superimposed on the quasi-static electric field enhancement (red line). (top right) A similar example of a high-level discharge activity superimposed on a quasi-static electric field was recorded near Rustrel (43.9°N, 5.5°E) in southeastern France on 30 August 2012, 03:33:46 UTC. (middle) The quasi-static electric field is dissipated during the high-level discharge activity as measured by the electric field variability ΔE. (bottom) The high-level discharge activity occurs within the thundercloud at an altitude range ~2–5 km as mapped by a small-scale interferometric network of four radio receivers deployed near Rustrel.

results in the dielectric breakdown ~15–20 km away from the sprite group. This breakdown thereby illuminates the mesospheric irregularity, i.e., a luminous patch which occupies a volume ~3–19 km^3. A weak negative lightning discharge initiates the rebrightening of the mesospheric irregularity, and the consecutive intracloud lighting discharges reorganize the charge distribution inside the thundercloud to compensate for the new charge configuration. This reorganization of charge results in a quasi-static electric field which causes the patch of mesospheric irregularity to develop into a columniform streamer which slowly descends at a speed of ~1.25–$2.50 \cdot 10^5$ m s^{-1}. The charge moment Ql which causes the quasi-static electric field E can be inferred from the maximum-observed electric field ~0.4 V m^{-1} by use of the standard description for electrostatic fields

$$E = \frac{2Ql}{4\pi\varepsilon_0(l^2 + d^2)^{3/2}} \qquad (2)$$

[*Uman*, 1987, equation A.3, p. 315], where Q is the amount of charge at an average height l above the ground, ε_0 is the electric field constant, and d is the horizontal distance between the charge and the receiver. Assuming that the charge causing the quasi-static electric field is located near the mixed phase region of the thundercloud ~4–6 km height and that the horizontal distance is the same as the distance to the positive lightning discharge ~77 ± 20 km results in a charge moment ~4–20 C km. This is more than one order of magnitude below the charge moment ~600 C km which is typically required for the inception of sprites [*Qin*

et al., 2012a; *Cummer and Lyons*, 2005] and one order of magnitude below the charge moment ~200–230 C km observed here, which initiates the sprite group. However, this small charge moment ~4–20 C km does not reflect inception because it is only required to sustain the downward propagation of the columniform streamer which is also assisted by the radiated field from the high-level activity of intracloud discharges. Several other weak negative lightning discharges with small peak currents occur at scattered locations around the positive lightning discharge (not shown in Figure 1) without having any observable effect on the mesosphere above. As a result, the initial luminous patch is almost certainly produced by a localized concentration of electric field lines causing an enhancement of the electric field strength, which results in a small-scale dielectric breakdown of mesospheric air and thereby illuminates the mesospheric irregularity.

4. Discussion

[9] The excellent agreement between the quasi-static electric field enhancement and the intensity of the intracloud discharges does not offer any information on cause and effect. The chosen interpretation is based on the idea that the intracloud discharges drive the quasi-static electric field enhancement. However, the ongoing discussion on the initiation of lightning discharges during preliminary breakdown [*Gurevich et al.*, 2013; *Gurevich and Karashtin*, 2013; *Dwyer*, 2012, 2005; *Gurevich et al.*, 1992] is based on the

idea that streamer like microdischarges inside thunderclouds are caused by a preexisting quasi-static electric field. This line of thought would require a physical mechanism which causes the observed rise and decay of the quasi-static electric field. One possible mechanism could be for example electron pileup during which the positive cloud-to-ground discharge dislocates electrons with the heavier ions following later to neutralize the electric field produced by the dislocated electrons. Such kind of mechanism could be in operation, for example, if hydrometeors [*Gurevich et al.*, 2013; *Gurevich and Karashtin*, 2013] or aerosols [*Füllekrug et al.*, 2013, 2013b] contribute significantly to the observed quasi-static electric field.

[10] Quasi-static electric field measurements of sprites have previously been attributed to radiating current flowing in the body of the sprite [*Hager et al.*, 2012]. It is therefore interesting to estimate the charge per unit length, or line charge, of the descending column sprite because no long-range electromagnetic radiation is observed in this study. In this case, the maximum electric field is given by

$$E = \frac{2}{4\pi\varepsilon_0} \int_{h_1}^{h_2} \frac{\rho z}{(z^2 + d^2)^{3/2}} \, \mathrm{d}z = \frac{2\rho}{4\pi\varepsilon_0} \left[-\frac{1}{\sqrt{z^2 + d^2}} \right]_{h_1}^{h_2} \quad (3)$$

[*Uman*, 1987, equation A.8, p. 317], where ρ is the average line charge along the length z extending from the bottom height $h_1 \approx 75$ km to the top height $h_2 \approx 85$ km of the columniform sprite at the time of maximum luminosity. The line charge stored on mesospheric aerosols or hydrometeors could then be as large as $\sim$30–60 μC m^{-1} assuming that the horizontal distance d to the columniform sprite is the same as the distance to the positive lightning discharge $\sim$77$\pm$20 km. The inferred mesospheric line charge is one order of magnitude smaller than the line charge of a stratospheric leader stem in a gigantic jet [*Neubert et al.*, 2011], and it is hence indicative of a weak sprite. The observed quasi-static electric field could also result from a preceding halo [*Bennett and Harrison*, 2013; *Parra-Rojas et al.*, 2013; *Kuo et al.*, 2013], a bidirectional leader [*Mallios et al.*, 2013], or a resurgent lightning continuing current [*Yashunin et al.*, 2007]. However, all these processes would radiate electromagnetic waves to long-range distances which are not observed in this study.

[11] The theoretical modeling of sprite initiation suggests enhancements of the ambient electron density by one order of magnitude which possibly result from ionospheric disturbances by meteor trails, electrodynamic effects from thunderstorms and lightning, or gravity wave breaking [*Qin et al.*, 2013a; *Kosar et al.*, 2012] which are occasionally observed as irregular luminosities of elves and halos [*van der Velde et al.*, 2011] and might assist sprite initiation [*Moudry et al.*, 2003]. Electron density enhancements effectively concentrate the electric field lines and thereby increase the local electric field strength, which increases the likelihood for dielectric breakdown to occur. Electric field lines can also be concentrated at the surface of ambient air impurities such as solid particulates, e.g., iron from meteor ablation [*Feng et al.*, 2013; *Gabrielli et al.*, 2004; *Rapp and Lübken*, 2004] or ice crystals [*Rapp and Thomas*, 2006]. In either case, such kind of mesospheric irregularities near the mesopause would be illuminated by the electromagnetic field of lightning discharges as observed here.

[12] The detected mesospheric irregularity illuminates a maximum volume of $\sim$3–19 km^3 which is considered to be an upper bound as a result of the limited spatial and temporal resolution of the video images. For example, the initial luminous patch could result from a prompt column sprite with a typical width $\sim$0.2–0.6 km [*McHarg et al.*, 2010] which propagates downward at a velocity $\sim$1–10$\cdot$10^6 m s^{-1} [*Li and Cummer*, 2009] to reach a vertical extent of $\sim$4–6 km within $\sim$0.5–5 ms before it collapsed, such that the mesospheric irregularity would only account for some fraction of the observed luminosity. On the other hand, the horizontal extent of the patch $\sim$1–2 km and the downward propagation speed $\sim$1.25–2.50$\cdot$10^5 m s^{-1} during the rebrightening of the patch suggests that the mesospheric irregularity could occupy a volume up to $\sim$19 km^3 to account for all of the observed luminosity. In either case, the concentration of the electric field lines by the mesospheric irregularity at a significant distance from the sprite group effectively acts as an inception point for dielectric breakdown to occur, similar to the scattered inception points reported in association with a column and carrot sprite [*Qin et al.*, 2013b, Figure 1].

[13] Such mesospheric irregularities would be particularly effective in the absorption and scattering of radio waves with comparable wavelengths in the frequency range of hundreds of kilohertz which are used for the delivery of applications, e.g., atomic time transfer and marine navigation [*Mezentsev and Füllekrug*, 2013] remaining to be investigated in future studies.

5. Summary

[14] In summary, a mesospheric irregularity is illuminated by the electromagnetic pulse of an intense positive cloud-to-ground lightning discharge. A consecutive weak negative lightning discharge initiates the rebrightening of the irregularity which develops into a slowly descending columniform sprite assisted by a quasi-static electric field enhancement which is driven by a high level of intracloud lightning discharge activity. Future studies on the illumination of mesospheric irregularities by lightning discharges could make use of video cameras with a smaller noise level of the recording chip, sampling at higher frequencies, and use telescopic imaging to focus around the mesopause region. Such kind of experimental scientific program might assist an improved understanding of the absorption and scattering of 100 kHz radio waves which are used for the delivery of applications such as atomic time transfer and marine navigation.

[16] The Editor thanks two anonymous reviewers for their assistance in evaluating this paper.

References

Bennett, A., and R. Harrison (2013), Lightning-induced extensive charge sheets provide long range electrostatic thunderstorm detection, *Phys. Rev. Lett.*, *111*(4), 045,003, doi:10.1103/PhysRevLett.111.045003.

Blanc, E., F. Lefeuvre, R. Roussel-Dupré, and J. Sauvaud (2007), TARANIS: A microsatellite project dedicated to the study of impulsive transfers of energy between the Earth atmosphere, the ionosphere, and the magnetosphere, *Adv. Space Res.*, *40*(8), 1268–1275, doi:10.1016/j.asr.2007.06.037.

Cummer, S., and W. Lyons (2005), Implications of lightning charge moment changes for sprite initiation, *J. Geophys. Res.*, *110*, A04304, doi:10.1029/2005JA010812.

Dwyer, J. (2005), The initiation of lightning by runaway air breakdown, *Geophys. Res. Lett.*, *32*, L20808, doi:10.1029/2005GL023975.

Dwyer, J. (2012), The relativistic feedback discharge model of terrestrial gamma ray flashes, *J. Geophys. Res.*, *117*, A02308, doi:10.1029/2011JA017160.

Feng, W., D. Marsh, M. Chipperfield, D. Janches, J. Höffner, F. Yi, and J. Plane (2013), A global atmospheric model of meteoric iron, *J. Geophys. Res. Atmos.*, *118*, 9456–9474, doi:10.1002/jgrd.50708.

Füllekrug, M. (2010), Wideband digital low-frequency radio receiver, *Meas. Sci. Technol.*, *21*(1), 015,901, doi:10.1088/0957-0233/21/1/015901.

Füllekrug, M., and S. Reising (1998), Excitation of Earth-ionosphere cavity resonances by sprite-associated lightning flashes, *Geophys. Res. Lett.*, *25*(22), 4145–4148.

Füllekrug, M., and M. Rycroft (2006), The contribution of sprites to the global atmospheric electric circuit, *Earth Planets Space*, *58*(9), 1193–1196.

Füllekrug, M., M. Ignaccolo, and A. Kuvshinov (2006), Stratospheric joule heating by lightning continuing current inferred from radio remote sensing, *Radio Sci.*, *41*, RS2S19, doi:10.1029/2006RS003472.

Füllekrug, M., et al. (2013), Electron acceleration above thunderclouds, *Environ. Res. Lett.*, *8*, 035,027, doi:10.1088/1748-9326/8/3/035027.

Füllekrug, M., et al. (2013b), Energetic charged particles above thunderclouds, *Surv. Geophys.*, *34*(1), 1–41, doi:10.1007/s10712-012-9205-z.

Gabrielli, P., et al. (2004), Meteoric smoke fallout over the holocene epoch revealed by iridium and platinum in Greenland ice, *Nature*, *432*(7020), 1011–1014, doi:10.1038/nature03137.

Gamerota, W., S. Cummer, J. Li, H. Stenbaek-Nielsen, R. Haaland, and M. McHarg (2011), Comparison of sprite initiation altitudes between observations and models, *J. Geophys. Res.*, *116*(A2), A02317, doi:10.1029/2010JA016095.

Gonzalez, R., and R. Woods (2008), *Digital Image Processing*, Prentice Hall, Englewood Cliffs, N. J.

Gurevich, A., and A. Karashtin (2013), Runaway breakdown and hydrometeors in lightning initiation, *Phys. Rev. Lett.*, *110*(18), 185,005, doi:10.1103/PhysRevLett.110.185005.

Gurevich, A., G. Milikh, and R. Roussel-Dupré (1992), Runaway electron mechanism of air breakdown and preconditioning during a thunderstorm, *Phys. Lett. A*, *165*, 463–468, doi:10.1016/0375-9601(92)90348-P.

Gurevich, A., et al. (2013), Correlation of radio and gamma emissions in lightning initiation, *Phys. Rev. Lett.*, *111*(16), 165,001, doi:10.1103/PhysRevLett.111.165001.

Hager, W., et al. (2012), Charge rearrangement by sprites over a north Texas mesoscale convective system, *J. Geophys. Res.*, *117*(D22), D22101, doi:10.1029/2012JD018309.

Hu, W., S. Cummer, and W. Lyons (2007), Testing sprite initiation theory using lightning measurements and modeled electromagnetic fields, *J. Geophys. Res.*, *112*(D13), D13115, doi:10.1029/2006JD007939.

Kosar, B., N. Liu, and H. Rassoul (2012), Luminosity and propagation characteristics of sprite streamers initiated from small ionospheric disturbances at subbreakdown conditions, *J. Geophys. Res.*, *117*(A8), A08328, doi:10.1029/2012JA017632.

Kuo, C., et al. (2013), Ionization emissions associated with N_2^+ 1N band in halos without visible sprite streamers, *J. Geophys. Res. Space Physics*, *118*, 5317–5326, doi:10.1002/jgra.50470.

Lefeuvre, F., E. Blanc, J. Pinçon, R. Roussel-Dupré, D. Lawrence, J. Sauvaud, J. Rauch, H. Feraudy, and D. Lagoutte (2008), TARANIS—A satellite project dedicated to the physics of TLEs and TGFs, *Space Sci. Rev.*, *137*(1–4), 301–315, doi:10.1007/s11214-008-9414-4.

Li, J., and S. Cummer (2009), Measurement of sprite streamer acceleration and deceleration, *Geophys. Res. Lett.*, *36*(10), L10812, doi:10.1029/2009GL037581.

Li, J., S. Cummer, W. Lyons, and T. Nelson (2008), Coordinated analysis of delayed sprites with high-speed images and remote electromagnetic fields, *J. Geophys. Res.*, *113*(D20), D20206, doi:10.1029/2008JD010008.

Liu, N., B. Kosar, S. Sadighi, J. Dwyer, and H. Rassoul (2012), Formation of streamer discharges from an isolated ionization column at subbreakdown conditions, *Phys. Rev. Lett.*, *109*(2), 025,002, doi:10.1103/PhysRevLett.109.025002.

Mallios, S., S. Celestin, and V. Pasko (2013), Production of very high potential differences by intracloud lightning discharges in connection with terrestrial gamma ray flashes, *J. Geophys. Res. Space Physics*, *118*, 912–918, doi:10.1002/jgra.50109.

McHarg, M., H. Stenbaek-Nielsen, T. Kanmae, and R. Haaland (2010), Streamer tip splitting in sprites, *J. Geophys. Res.*, *115*, A00E53, doi:10.1029/2009JA014850.

Mezentsev, A., and M. Füllekrug (2013), Mapping the radio sky with an interferometric network of low-frequency radio receivers, *J. Geophys. Res. Atmos.*, *118*, 8390–8398, doi:10.1002/jgrd.50671.

Moudry, D., H. Stenbaek-Nielsen, D. Sentman, and E. Wescott (2003), Imaging of elves, halos and sprite initiation at 1 ms time resolution, *J. Atmos. Sol. Terr. Phys.*, *65*, 509–518, doi:10.1016/S1364-6826(02)00323-1.

Neubert, T., O. Chanrion, E. Arnone, F. Zanotti, S. Cummer, M. Füllekrug, S. Soula, and O. van der Velde (2011), The properties of a gigantic jet reflected in a simultaneous sprite: Observations interpreted by a model, *J. Geophys. Res.*, *116*(A12), A12329, doi:10.1029/2011JA016928.

Parra-Rojas, F., A. Luque, and F. Gordillo-Vázquez (2013), Chemical and electrical impact of lightning on the Earth mesosphere: The case of sprite halos, *J. Geophys. Res. Space Physics*, *118*, 5190–5214, doi:10.1002/jgra.50449.

Qin, J., S. Celestin, and V. Pasko (2012a), Minimum charge moment change in positive and negative cloud to ground lightning discharges producing sprites, *Geophys. Res. Lett.*, *39*(22), L22801, doi:10.1029/2012GL053951.

Qin, J., S. Celestin, and V. Pasko (2012b), Formation of single and double-headed streamers in sprite-halo events, *Geophys. Res. Lett.*, *39*(5), L05810, doi:10.1029/2012GL051088.

Qin, J., S. Celestin, and V. Pasko (2013a), Dependence of positive and negative sprite morphology on lightning characteristics and upper atmospheric ambient conditions, *J. Geophys. Res. Space Physics*, *118*, 2623–2638, doi:10.1029/2012JA017908.

Qin, J., S. Celestin, V. Pasko, S. Cummer, G. McHarg, and H. Stenbaek-Nielsen (2013b), Mechanism of column and carrot sprites derived from optical and radio observations, *Geophys. Res. Lett.*, *40*(17), 4777–4782, doi:10.1002/grl.50910.

Rapp, M., and F. Lübken (2004), Polar mesosphere summer echoes (PMSE): Review of observations and current understanding, *Atmos. Chem. Phys.*, *4*, 2601–2633, doi:10.5194/acp-4-2601-2004.

Rapp, M., and G. Thomas (2006), Modeling the microphysics of mesospheric ice particles: Assessment of current capabilities and basic sensitivities, *J. Atmos. Sol. Terr. Phys.*, *68*, 715–744, doi:10.1016/j.jastp.2005.10.015.

Soula, S., et al. (2012), Multi-instrumental analysis of large sprite events and their producing storm in southern France, *Atmos. Res.*, *135–136*, 415–431, doi:10.1016/j.atmosres.2012.10.004.

Uman, M. (1987), *The Lightning Discharge*, Academic Press, New York.

van der Velde, O., J. Montanyá, S. Soula, N. Pineda, and J. Bech (2010), Spatial and temporal evolution of horizontally extensive lightning discharges associated with sprite-producing positive cloud-to-ground flashes in northeastern Spain, *J. Geophys. Res.*, *115*(A9), A00E56, doi:10.1029/2009JA014773.

van der Velde, O., J. Montanyá, M. Füllekrug, and S. Soula, (2011), Gravity waves, meteor trails and asymmetries in elves, *ICAE Conference Report*, Rio de Janeiro, Brazil.

Yashunin, S., E. Mareev, and V. Rakov (2007), Are lightning M components capable of initiating sprites and sprite halos?, *J. Geophys. Res.*, *112*(D10), D10109, doi:10.1029/2006JD007631.